

1 **Methods for Reducing Biases and Errors in Regional**
2 **Photochemical Model Outputs for Use in Emission**
3 **Reduction and Exposure Assessments**
4
5

6 P. Steven Porter¹, S. Trivikrama Rao², Christian Hogrefe³, Edith Gego¹, Rohit
7 Mathur³
8

9 ¹Porter-Gego, Idaho Falls, ID 83401

10 ²North Carolina State University, Raleigh, NC 27695

11 ³US EPA National Exposure Research Laboratory, Research Triangle Park, NC
12 27711
13
14

15 **Abstract**
16

17 In the United States, regional-scale photochemical models are being used to design emission
18 control strategies needed to meet the relevant National Ambient Air Quality Standards (NAAQS)
19 within the framework of the attainment demonstration process. Previous studies have shown that
20 the current generation of regional photochemical models can have large biases and errors in
21 simulating absolute levels of pollutant concentrations. Studies have also revealed that regional
22 air quality models were not always accurately reproducing even the relative changes in ozone air
23 quality stemming from changes in emissions. This paper introduces four approaches to adjust for
24 model bias and errors in order to provide greater confidence for their use in estimating future
25 concentrations as well as using modeled pollutant concentrations in exposure assessments. The
26 four methods considered here are a mean and variance (MV) adjustment, temporal component
27 decomposition (TC) adjustment of modeled concentrations, and two variants of cumulative
28 distribution function (CDF) mapping. These methods were compared against each other as well
29 as against unadjusted model concentrations and a version of the relative response approach based
30 on unadjusted model predictions. The analysis uses ozone concentrations simulated by the

31 Community Multiscale Air Quality (CMAQ) model for the northeastern United States domain
32 for the years 1996 to 2005. Ensuring that base case conditions are adequately represented
33 through the combined use of observations and model simulations is shown to result in improved
34 estimates of future air quality under changing emissions and meteorological conditions.

35 _____

36 Corresponding Author: Dr. S.T. Rao (strao@ncsu.edu)

37 Key Words: Air quality Modeling, Model Evaluation, Bias Adjustment, Emission Control
38 Strategy Assessment, Attainment Demonstration, Exposure Assessment

39 **1. Introduction**

40

41 Regional-scale photochemical models are useful tools for forecasting (Eder et al., 2010),
42 regulatory decision-making (USEPA, 2014), and exposure assessments (Garcia et al., 2010; Lin
43 et al., 2012). Forecasts of future air quality enable people to take appropriate precautionary
44 measures to reduce their exposure to high pollution levels (Eder et al., 2010). With respect to
45 exposure assessments, it is desirable to relate air quality to human health at unmonitored
46 locations (Garcia et al., 2010; Lin et al., 2012) and to deal with missing data at monitoring sites
47 (i.e., Junninen et al., 2004). Spatially and temporally dense model outputs, adjusted for biases in
48 mean and variability are used for these purposes. Attainment demonstrations use a set of model
49 experiments to assess the magnitude and extent of air pollution and to determine emission
50 reductions needed to meet the National Ambient Air Quality Standards (NAAQS). In particular,
51 models are used to compare past air quality (base case) with model-predicted future conditions.
52 This paper addresses the use of models in attainment demonstrations and exposure assessments.

53

54 Before a regional photochemical model is applied in the regulatory setting, USEPA's guidance
55 for the attainment demonstration recommends a thorough evaluation of the model performance
56 for the base case simulation (USEPA, 2014). Sistla et al. (2004), Jones et al. (2005), Pegues et
57 al. (2012), Hogrefe et al. (2012), Kulkarni et al. (2014), and Cohan and Chen (2014) have
58 examined some issues with the use of projected design values in attainment demonstrations.
59 Dennis et al. (2010) provided a framework for performing comprehensive model evaluation,
60 which entails conducting operational (Appel et al., 2007), dynamic (Napelenok et al., 2011),
61 diagnostic (Godowitch et al., 2011), and probabilistic evaluations (Hogrefe and Rao, 2001; Foley

62 et al., 2012; Reich et al., 2013). Also, scientists from North America and Europe have been
63 helping advance the model evaluation framework outlined by Dennis et al. (2010) as part of the
64 Air Quality Modelling Evaluation International Initiative (AQMEII) project (Rao et al., 2011;
65 Galmarini et al., 2012). The AQMEII community is currently focusing on evaluating the
66 performance of coupled meteorology and atmospheric chemistry models (Baklanov et al., 2014)
67 to examine the strengths and limitations of air quality models being used in North America and
68 Europe. In addition, techniques such as Kalman filtering (Delle Monache, 2006; Kang et al.,
69 2008 and 2010) and spectral decomposition approach (Galmarini et al., 2013) have been used to
70 correct for model bias in air quality forecasting.

71
72 It is important to promote model evaluations to establish credibility for air quality models so they
73 can be more confidently used for regulatory decisions. However, despite continual improvement
74 in models, discrepancies between model predictions and observations persist, stemming from
75 both reducible and irreducible errors. In addition, whereas modeled concentrations represent
76 volume-average concentrations, observations reflect point measurements at a given location.
77 Also, the stochastic variations affecting the monitored concentrations are not explicitly modeled
78 in the current regional numerical air quality models. Reducible errors (structural and parametric)
79 are attributable to our inadequate understanding of the relevant atmospheric processes, and errors
80 in model input variables (e.g., emissions, meteorology, boundary conditions, physics and
81 chemistry). Irreducible errors arise from our inability to properly characterize the initial state as
82 well as the stochastic nature of the atmosphere. A critical point to bear in mind is that it is
83 difficult, if not impossible, to specify the atmospheric conditions (i.e., emissions, initial and
84 boundary conditions, meteorology, physics, and chemistry) that real-world observations are

85 seeing in all locations at all times by simulating the base case conditions using air quality
86 models. In consequence, modeled pollutant concentrations often are biased (average observed
87 values are not reproduced) (Simon et al., 2012), exhibit less variability than the corresponding
88 observations (i.e., the distribution of modeled values is often more narrow than that of the
89 observations), and show changes in pollutant levels from the base case that differ from observed
90 changes (Gilliland et al., 2008; Godowitch et al., 2010). One way to address these limitations is
91 to constrain the model output by the observations to ensure that observations and modeled values
92 are starting from the same point so the deviations from the base case can be properly evaluated
93 as emissions and/or meteorology are altered. It should be emphasized that this does not imply
94 that scientific advances for better simulating the interactions of pollutants and transport and fate
95 in the atmosphere are not needed.

96

97 In an attempt to better meet the needs of regulatory agencies as well as the health sciences
98 community for regional air quality models, we propose four new methods for bringing the
99 statistical properties (i.e., mean, variance, percentiles) of model predictions into closer harmony
100 with pollutant concentrations observed at monitoring sites. Included are adjustments to the
101 concentration time series (matching the mean and variance of model ozone time series to
102 observations), spectral decomposition of time series (matching the low and high frequency
103 variations in model ozone time series to observations), and two variations of cumulative
104 distribution function (CDF) matching (matching sample CDFs of modeled and observed
105 concentrations, disregarding the time sequence). A ten-year long photochemical model
106 simulation for the northeastern USA is used to assess the performance of these methods. The
107 ability of these methods to reproduce different-year ozone concentrations as well as

108 contemporaneous predictions, that is, same-year ozone concentration time series, is evaluated.
109 The new approaches are compared with absolute model projections and with model-based,
110 relative response factors based on unadjusted model predictions.

111

112

113 **2. Data and Methods**

114

115 **A. Model Setup**

116

117 The following is a brief summary of the model set-up used to perform the simulations analyzed
118 in this study. The reader is referred to Hogrefe et al. (2009, 2010) for additional details. The
119 Mesoscale Meteorological Model MM5 (Grell et al., 1994) was used to simulate meteorological
120 conditions for the time period from 1 January 1988 to 31 December 2005. In the current study,
121 we utilize model simulations for the ten year period from 1996 to 2005. The meteorological
122 simulations were performed on two-way nested grids with 36 km and 12 km grid cell sizes
123 covering the northeastern US. Throughout the model simulation, MM5 was nudged towards
124 reanalysis fields from the National Center for Environmental Prediction (NCEP) using four-
125 dimensional data assimilation. All emission processing, including mobile and biogenic sources,
126 was performed within the Sparse Matrix Operator Kernel Emissions (SMOKE) system
127 (Houyoux et al., 2000). Anthropogenic emission inventories for 1988–2005 were compiled from
128 a variety of sources as described in Hogrefe et al. (2009). Various regulatory control programs
129 were implemented for the utility sector (e.g., the acid rain control program, NO_x SIP Call)
130 during the period 1995 to 2005. Also, fleet turnover has contributed to large changes in mobile

131 source emissions and control programs were also implemented for a number of other emission
132 sources. The combined effect of all emission control programs was a decrease of domain-wide
133 anthropogenic NO_x and VOC emission by roughly 24% and 28%, respectively during the 1996-
134 2005 period. Biogenic emissions were estimated with the BEIS3.12 model (Pierce et al., 1998)
135 taking into account MM5 temperature, radiation, and precipitation.

136
137 Regional air quality simulations were performed with the Community Multiscale Air Quality
138 (CMAQ) model (Byun and Schere, 2006), version 4.6, rather than CMAQ 4.5.1 that was used in
139 Hogrefe et al. (2009) with the same set of meteorological and emission inputs. Air quality model
140 simulations were performed with two one-way nested grids of 36 km and 12 km, corresponding
141 to the MM5 grids except for a ring of buffer cells. The height of the first model layer was set at
142 38 m. Gas phase chemistry was represented by the CB-IV mechanism (Gery, 1989) while
143 aerosol chemistry was simulated with the “aero3” module. In this study, only results from the 12
144 km CMAQ simulations were utilized. Chemical boundary conditions for the 36 km grid were
145 extracted from archived monthly-mean fields of global chemistry simulations performed for the
146 1988–2005 time period with the ECHAM5-MOZART modeling system as part of the RETRO
147 project (RETRO, 2007). The MM5/CMAQ simulations for this paper have been evaluated
148 against observations in Hogrefe et al. (2009, 2010) and Civerolo et al. (2010).

149

150 **B. Observations**

151

152 Hourly ozone observations during 1996-2005 were extracted from the USEPA’s Air Quality
153 System (AQS) (<http://www.epa.gov/ttn/airs/airsaqs/detaildata/downloadaqdata.htm>).

154 From these hourly data, daily maximum 8-hr average ozone concentration time series for each
155 ozone season (May 1 – September 30) and year were developed and screened to ensure that all
156 stations used in this analysis had at least 80% data completeness for any given ozone season and
157 year.

158

159 **C. Adjustment Methods**

160

161 *(1) RATIO*

162

163 The USEPA-recommended use of models in an attainment demonstration (USEPA, 2014) is
164 based on an assumption that the ratio of future case model simulations to base case model
165 simulations averaged over high simulated ozone days is a good predictor of changes in observed
166 ozone design values. Model predictions for the future year are usually a combination of past
167 meteorology and future emission scenarios needed to reduce ozone concentrations in non-
168 attainment areas.

169

170 $DVF = DVC \bullet RRF$ (1)

171

172 DVF = Design Value for the Future Year

173 DVC = Design Value for the Current Year

174 RRF = Relative Response Factor

175

176 As detailed in USEPA (2007), the calculation of the DVC is based on multiple years of observed
177 data while the RRF is calculated from averaged model simulations for both emission scenarios
178 under the same meteorological conditions following a specified set of criteria. *This calculation is*
179 *based on a combination of past meteorology and future emissions, which cannot be verified*
180 *because future year meteorology cannot be known and there are no comparable future*
181 *observations available for model adjustments.* In this study, we examine a simple ratio method
182 (hereafter referred to as the RATIO method) based on a single year of observations and non-
183 averaged model predictions for the base case and future case:

184

185 $future\ prediction = observed\ base \times \frac{CMAQ\ future\ year}{CMAQ\ base\ year}$ (2)

186

187 For example, when applying the RATIO method, defined in Eq (2), to project the future year 4th
188 highest daily maximum 8-hr ozone (4HDM8O3) concentration, one would multiply the observed
189 base year 4HDM8O3 concentration with the ratio of CMAQ predicted 4HDM8O3
190 concentrations for the future and base year. Like the RRF approach described in USEPA (2007),
191 the RATIO approach assumes that model predictions can be used in a relative sense; that is, even
192 though the absolute levels of modeled concentrations may be biased, they can be used to predict

193 the change in pollution levels from a given scenario. In contrast to the approach outlined in
194 USEPA (2007), the CMAQ base year and future year simulations analyzed in this study reflect
195 changes in both emissions and meteorology while in typical attainment demonstrations, the base-
196 year meteorological conditions are used for both the base year and future year when calculating
197 RRFs because the future year meteorology cannot be known. Also, given the uncertainties
198 associated with estimating future year modeled concentrations, the EPA approach is intended to
199 estimate multi-year average design values. The EPA approach does not attempt to precisely
200 predict 4HDM8O3 concentrations. Because meteorology is not held constant in the RATIO
201 approach, it can be verified via a simulation of ozone for the northeastern U.S. for the years 1996
202 to 2005.

203
204 Figure 1 presents an illustrative test of the RATIO approach for an arbitrary base year / future
205 year combination selected from the observational and model database described in the previous
206 section. This figure depicts the observed and CMAQ ratios of future year (2004) to base year
207 (2001) 4HDM8O3 concentrations at all (80% complete) monitoring sites in the modeling domain
208 along with the 1-to-1 line. CMAQ typically underestimates observed changes (Gilliland et al
209 2008; Godowitch, et al., 2010; Napelenok et al. 2011). The large scatter evident in this figure
210 suggests that it is worth investigating potential alternatives to the RATIO approach that may
211 provide better performance in predicting 4HDM8O3 concentrations into the future.

212

213 ***(2) Mean and Variance matching (MV)***

214

215 For each ozone season, we adjust the mean and variance of the modeled 8-hour ozone time series
 216 (i.e., the daily maximum 8-hr average ozone time series) so that they match those observed:

$$217 \quad \mathbf{future\ prediction} = \quad \mathbf{mean}\ \{\mathbf{CMAQ\ future}\} + \quad \quad \quad \mathbf{(3)}$$

$$218$$

$$219 \quad \quad \quad \{\mathbf{CMAQ\ future} - \mathbf{mean\ CMAQ\ future}\} \times \frac{\sigma(\mathbf{observed\ base\ year})}{\sigma(\mathbf{CMAQ\ base\ year})}$$

$$220$$

$$221 \quad \quad \quad + \mathbf{mean}\ \{\mathbf{observed\ base\ year} - \mathbf{CMAQ\ base\ year}\}$$

222

223 Base year adjustment factors (ratio of standard deviations and the mean bias) computed for each
 224 ozone season (153 days) are applied to other ozone seasons (**prediction** years). The **prediction**
 225 year 4HDM8O3 is then compared with that observed. The rationale for this method is that the
 226 distribution of CMAQ ozone is typically narrower than that observed (see Figure 7 in section 3)
 227 because modeled values reflect grid volume averages while observations represent discrete point
 228 measurements.

229

230 **(3) Mean and Variance matching with temporal components (TC)**

231

232 In this approach, mean and variance matching are applied to temporal components of modeled
 233 and observed values. Temporal components in this case are high- and low-frequency variation
 234 (denoted ‘HF and ‘LF’, respectively). The LF component is the output of a low-pass filter (i.e.,
 235 the KZ filter with a window size of five (5) days and five (5) iterations, and a 50% cutoff period
 236 of about 24 days, Rao and Zurbenko, 1994), while the HF component is the difference between

237 observations and the LF component (and therefore has a mean of zero). The period of separation
 238 between the HF and LF components is roughly 24 days.

239

240 The adjusted CMAQ values are given by:

241

$$242 \quad \mathbf{observed (base year)} = \mathbf{observed (LF, base year)} + \mathbf{observed(HF, base year)} \quad (4)$$

243

$$244 \quad \mathbf{CMAQ} = \mathbf{CMAQ(LF)} + \mathbf{CMAQ(HF)} \quad (5)$$

245

246 The principle behind this approach is that low- and high-frequency processes are driven by
 247 different phenomenon, with high-frequency variation attributable primarily to the synoptic-scale
 248 weather (i.e., variations due to fast changing emissions, diurnal forcing, and weather-induced
 249 variations embedded in ozone time series data), and low-frequency variation driven by seasonal
 250 emissions and trends (Rao et al., 1997). It follows that components with different driving forces
 251 should have different adjustments. Therefore, we adjust the mean and variance of each
 252 component of the modeled daily maximum 8-hr ozone time series so that they match those
 253 observed:

$$254 \quad \mathbf{future (LF)} = \quad \mathbf{mean \{CMAQ future LF\}} + \quad (6)$$

255

$$256 \quad \mathbf{\{CMAQ future LF - mean CMAQ future LF\}} \times \frac{\mathbf{\sigma(observed base year LF)}}{\mathbf{\sigma(CMAQ base year LF)}}$$

257

$$258 \quad \mathbf{+ mean \{observed base year LF - CMAQ base year LF\}}$$

259

260

261

$$262 \quad \mathbf{future (HF)} = \mathbf{CMAQ future HF} \times \frac{\sigma(\mathbf{observed base year HF})}{\sigma(\mathbf{CMAQ base year HF})} \quad (7)$$

263

264

$$265 \quad \mathbf{future} = \mathbf{future (LF)} + \mathbf{future (HF)} \quad (8)$$

266

267 As with the **MV** method, the **TC** method adjusts the entire time series (not just the 4th highest)
268 and assumes base year *variance ratios* and *mean bias* will be the same in future years for both
269 high- and low- frequency components.

270

271 **(4) Cumulative Distribution Function matching (CDF1)**

272 Cumulative distribution function matching (CDF matching) is a bias correction technique used in
273 climate data analysis and image processing (see Wang and Chen, 2014 for example). Observed
274 and modeled concentrations are rank-ordered to establish sample CDF's (sample quantiles). The
275 observed quantiles are regressed against those of CMAQ yielding the following:

$$276 \quad \mathbf{observed base year quantiles} = \mathbf{Ko} + \mathbf{K1} \bullet \mathbf{CMAQ base year quantiles} \quad (9)$$

$$277 \quad \mathbf{future quantiles} = \mathbf{Ko} + \mathbf{K1} \bullet \mathbf{CMAQ future quantiles}$$

278 The slope and intercept, **Ko** and **K1**, rotate and displace the CMAQ CDF such that the root mean
279 squared distance between the modeled and observed quantiles are minimized. The original time
280 order of CMAQ and observations is lost with this approach. As with methods 1 and 2, the

281 adjustment parameters estimated using base year observed and CMAQ information (in this case,
282 Ko and K₁) are applied to future years.

283

284 (5) *Cumulative Distribution Function matching (CDF2)*

285

286 In contrast with **CDF1**, the parameters Ko and K₁ in equation (11) are applied only to the base
287 year and the future year 4HDM8O3 concentration is estimated by adding the model predicted
288 change in 4HDM8O3 concentrations to the base year adjusted 4HDM8O3 concentration. As
289 with **CDF1**, the time order is lost.

$$290 \quad \text{Observed base year quantiles} = K_o + K_1 \bullet \text{CMAQ base year quantiles} \quad (10)$$

$$291 \quad \text{future quantiles} = \{\text{CMAQ future quantiles} - \text{CMAQ base year quantiles}\}$$

$$292 \quad \quad \quad +\{K_o + K_1 \bullet \text{CMAQ base year quantiles}\}$$

293

294 3. Results and Discussion

295

296 A. Predicting the 4th Highest Daily Maximum 8-hr Ozone Concentration

297

298 For every pair of years from 1996-2005, one year served as a base year and the other a prediction
299 year (a total of 90 pairs where the two years are different). For each *base year-prediction* year
300 pair, there are approximately 250 sites from which performance metrics were computed,
301 including mean bias (MB), fractional mean bias (FMB), mean absolute bias (MAB), fractional
302 MAB (FMAB), root mean squared error (RMSE), fractional RMSE (FRMSE), square of

303 correlation (R^2) and index of agreement (IA). As noted above, the quantity being evaluated in
304 this analysis is the 4HDM8O3 concentration.

305

306 Domain-wide RMSE, MAB, and R values, using 1996 as the base year for predicting the
307 4HDM8O3 for 1997 to 2005, are presented in Figure 2. There is a considerable amount of year-
308 to-year variation in the RMSE values, ranging from about 6 to 15 ppb. To provide a more
309 comprehensive evaluation of the different approaches, Table 1 provides the performance metrics
310 and their 95% bootstrap confidence intervals for predicting 4HDM8O3 concentrations for all
311 base year-prediction year pairs. From Figure 2, it is evident that no one method is best suited for
312 all the prediction years, but CDF2 often is the best among the six methods examined here for
313 predicting the 4HDM8O3 concentration. Table 1, with respect to the MAB metric on the basis
314 of overlapping confidence intervals, shows that, the MAB follows the order (TC, CDF1, CDF2)
315 $< MV < \text{RATIO} < \text{CMAQ}$, whilst for RMSE performance ranks are: (CDF1 , CDF2) , MV , (TC
316 , RATIO , CMAQ). For the other metrics (R^2 and IA) none of the methods stand out because all
317 the confidence intervals overlap. To help sort out these relationships, a multiple comparison for
318 all metrics MAB and RMSE (Table 2) also supports the conclusion that CDF1 and CDF2
319 perform better than RATIO and CMAQ methods.

320

321 The fact that the TC method has a higher RMSE, but not MAB, than the other methods both for
322 the 1996 base year (Figure 2) as well as all base year / future year pairs (Table 1) implies the
323 presence of outliers in the projected values that influence the RMSE metric to a greater degree
324 than the MAB metric.

325

326 Spatial images of the RMSE values for all base year / prediction year pairs at a given site,
327 displayed in Figure 3, indicate with the large number of red and orange dots that all methods
328 exhibit poorer performance at sites along the northeastern urban corridor (along interstate 95),
329 the northeastern seaboard, and near large water bodies. However, at many locations the four
330 adjustment methods introduced in this study tend to perform better in predicting 4HDM8O3
331 concentrations than the raw CMAQ output and RATIO approach. Table 3 shows the percentage
332 of pairwise counts for a given metric of ‘best’ results for all 90 base year / prediction year pairs.
333 Reading across row 1, for example, CMAQ has a lower MAB than RATIO and MV for 36% and
334 27% of the 90 pairs, respectively. For every metric, CDF2 and CDF1 are better than all other
335 methods for more than 50% of the pairs. CMAQ and RATIO are not better than any of the other
336 methods for more than 50% of the pairs. Thus, judging from the values of MAB, RMSE and
337 R^2 , CDF2 appears to be the best method among the four bias and error adjustments methods
338 considered here. However, it is evident from Table 1 that the differences in performance in
339 predicting the 4HDM8O3 values though often statistically significant are often small. For
340 example, RATIO has an RMSE of 9.5 ppb compared with CDF2 of 8.7 ppb.

341

342 As noted above, the EPA guidance recommends that a number of the highest ozone days be
343 averaged. Table 4 compares the adjustment methods when used with the highest ozone day up to
344 the average highest 10 days and with the 4th highest. *Averaging brings benefits to all the*
345 *methods discussed here, but the relative performance of each method is little changed.*

346

347 Next, we computed the frequency with which the predicted 4HDM8O3 concentration falls within
348 a specified range of the observed 4HDM8O3 concentrations across all sites and base-year /

349 prediction-year pairs. This metric can be thought of as the fraction of correct predictions.
350 Results depicted in Figure 4 show that all methods involving bias/error adjustments improve the
351 predictions of future 4HDM8O3 concentrations compared to the raw CMAQ output. Only 25%
352 of predictions fall within a target of 3% of observed 4HDM8O3's. While the CMAQ 4HDM8O3
353 concentrations are within 10% of the corresponding observations at 60% of the sites, CDF2 is
354 within 10% of the corresponding observations at 70% of the sites. As noted before, not all
355 monitoring sites in the model domain can be considered to be regionally-representative sites
356 since several sites are near urban areas or water bodies where regional scale air quality models
357 such as the 12 km CMAQ simulations used in this study cannot be expected to perform well
358 (Hogrefe et al., 2014).

359

360

361 RMSE values for the daily maximum 8-hr ozone concentrations predicted by the four methods
362 for the upper half of the distribution for the year 2004 using 2001 as the base year, presented in
363 Figure 5, reveal that all methods perform poorly in reproducing the observed concentrations for
364 the extreme values (upper percentiles >90%). Also, there is a large disparity between the
365 changes in absolute levels of CMAQ and observed ozone between 2001 and 2004 for the upper
366 half of the concentration frequency distribution (Fig.6a). The ozone improvement (the difference
367 in ozone concentrations between 2001 and 2004) simulated by CMAQ is much lower than that
368 seen in observations, especially in the upper percentiles (>75%). The difference is highlighted in
369 Fig. 6b which is a histogram of the change in ozone between 2001 and 2004 at the 98th percentile
370 for all monitors in the domain. Napelenok et al (2011) and Kang (2013) speculated that CMAQ
371 underestimation of ozone change is due to uncertainties in the NO_x emission inventory,

372 particularly mobile and area sources (because most point source emissions are measured by
373 continuous emission monitors found at electricity generating facilities).

374

375 Both Figures 6a and 6b reveal that all four bias and error adjustment methods tend to reduce the
376 discrepancy between the simulated and observed changes and help to bring the simulated change
377 in ozone between 2001 and 2004 closer to what was observed. It may be, then, that for
378 regulatory assessments (i.e., attainment demonstration), using observations to adjust base case
379 model bias and error leads to better estimates of future year design values than does use of the
380 original model values.

381

382 **B. Same-year Performance (demonstration of model's usefulness for exposure assessment)**

383 Spatially continuous time-series of air quality surfaces over large geographic regions are
384 desirable for assessments of the effects of chronic human exposure to air pollutants.

385 Photochemical models have been used for this purpose and it has been shown that their use in
386 conjunction with observations is an improvement over the use of observations alone (Garcia et
387 al, 2010). Put simply, model-observation bias is projected to unmonitored sites using
388 geostatistical methods. Modeled values for the gridded model domain are then adjusted using
389 the interpolated bias. Prediction of future (or past) times is usually not of interest (though
390 temporal interpolation may be). In this section, we suggest that model values adjusted via the
391 methods presented here may be an improvement over projecting model bias. A validation of the
392 use of adjusted values for exposure assessments will be addressed in a future paper.

393

394 As noted above, model probability distributions tend to be narrower than those observed (smaller
395 standard deviation and range). If modeled ozone values used in a health assessment have a
396 smaller range (or standard deviation) than what would be observed, the estimated health effect
397 will be biased. Many of the methods discussed here could be applied in same-year fashion to
398 model and observed information to help construct ozone fields or any pollutant species with
399 unbiased standard deviation.

400

401 As a first step in this direction, in this section, we evaluate ‘same-year’ performance for ozone
402 time series from raw CMAQ output, modeled ozone that is adjusted for bias and error using the
403 MV and TC methods, and modeled ozone that is adjusted using the CDF1 approach at the
404 discrete locations of the monitoring stations. By same-year it is meant that there is no projection
405 from base-year to prediction-year. Note that no results are computed in this section for the
406 RATIO and CDF2 approaches. For the RATIO approach, the same-year ratio of model
407 predictions shown in Eq (2) is equal to one, thus, predicted values would equal observed values;
408 for the CDF2 approach, the predicted value equals that for the CDF1 approach since the model
409 predicted differences between base-year and prediction-year are zero. The object of
410 investigating same-year performance, as noted above, is to test the potential usefulness of these
411 approaches for creating spatially continuous pollutant concentration time series that could be
412 used for exposure assessment.

413

414 Domain-wide statistics for (MAB, standard deviation, and correlation coefficient) for same-year
415 adjusted CMAQ values (annual 4th highest 8-hour daily maximum, 4HDM8O3) predictions were
416 computed for all years from 1996 – 2005. Results, depicted in Figures 7a-c, indicate TC and

417 CDF1 outperform MV and as expected the raw CMAQ. As noted above, an important criterion
418 for fitting exposure models is that the standard deviation of the adjusted values matches those
419 observed. As expected, standard deviations for the CDF1, MV, and TC methods closely match
420 the observed standard deviation while raw CMAQ underestimated the observed standard
421 deviation (Fig. 7b). That exposure assessment requires unbiased standard deviation estimates
422 was highlighted by NRC (2004). Therefore, a conclusion that can be reached from this study is
423 that raw CMAQ output should not be used for exposure assessments without some type of
424 bias/error-adjustment, and that the CDF1 and TC methods produces surrogate ozone time series
425 that, on average, are very close to the observed ozone time series. While CDF1 also exhibits
426 good performance as measured by these summary statistics, it does not retain the original time
427 order because it is designed to adjust the overall distribution rather than an adjusted
428 concentration time series. Thus, its potential use in health assessment studies would be limited to
429 analyses focused on long-term (chronic) rather than short-term (acute) exposures. The relative
430 performances of the three methods discussed above for reducing the bias in years 2001 and 2004
431 reveal the superior performance of the CDF1 and TC methods (Figs. 8) across a wide range of
432 percentiles, especially when compared to raw CMAQ output. However, it should also be noted
433 that the performance of all methods investigated here degrades at the very top end of the
434 concentration distribution (>90%). Nevertheless, the bias adjustment methods reduce the
435 magnitude of the error and bias present in the raw CMAQ output.

436

437 Since chronic exposure assessments rely on time series of pollutant concentrations, the TC
438 adjustment method appears to be the best approach; this is very useful information because
439 CMAQ output can be more confidently used for filling-in for the days when observations are not

440 available (see Junninen et al., 2004 for examples of data fill-in methods). For example, most
441 PM_{2.5} and speciated PM_{2.5} monitoring sites operate on a 1 in 3 day schedule. For the days with
442 missing data, the TC method can be used for correcting CMAQ output for bias and error so the
443 adjusted model output can be used to generate continuous pollutant time series for exposure
444 assessments by the health community. One could also adjust black carbon (BC) estimates or
445 other species simulated by CMAQ that are of particular interest to health scientists with one of
446 the above two methods to generate daily BC or other pollutant species time series for the whole
447 year for use in health risk assessments. Further steps then would be to spatially-interpolate the
448 adjusted ozone concentrations to the entire model domain using techniques such as those
449 suggested by Garcia et al. (2010), Macmillan (2010), Fuentes and Raftery (2005), and Crooks
450 and Isakov (2013).

451

452 **4. Summary**

453

454 Future year air quality predictions can be improved by adjusting for biased concentration
455 estimates while exposure assessments may also benefit from unbiased standard deviation
456 estimates. This paper discussed four methods for reducing the bias and errors in model predicted
457 pollutant concentrations so that the model can be more effectively used for both of these tasks.
458 Four methods were developed and tested using long-term modeling simulations for the
459 northeastern US domain. Three of the methods project base-year CMAQ bias metrics to
460 prediction-years. The projected metrics are (1) mean and variance, (2) mean and variance of
461 temporal components, and (3) regression parameters of a QQ plot. The fourth method uses QQ
462 plot regression parameters only for the base year. The methods were compared against

463 unadjusted model concentrations and model concentrations adjusted with a relative response
464 factor approach, similar in concept to what is typically used in attainment demonstrations to
465 estimate future air quality. Results demonstrate that the adjustment of modeled concentrations so
466 that they more closely resemble observations (i.e. the process of combining observations and
467 model predictions) usually improves the usefulness of CMAQ for both estimating future
468 concentrations stemming emission reduction policies and for conducting exposure assessments.
469 All adjustment methods were demonstrated to improve future year model estimates compared to
470 the absolute modeled projections. The following conclusions can be drawn based on the
471 performances of the methods considered here.

472

473 For estimating future year concentrations, the uncertainty in predicted changes in ozone levels
474 can be substantial and depends heavily on the particular locations and base- / prediction-year
475 pairs (recall Figure 1). Uncertainty estimates for predictions are unavailable without validation
476 studies based on multi-year modeling experiments. Methods that use the base year parameters
477 (MV, TC, and CDF1) to adjust prediction year model values are often less effective than
478 methods that do not (CDF2), suggesting that the characteristics of CMAQ's bias are non-
479 stationary. For exposure assessments, MV or TC adjustment methods applied to CMAQ model
480 output provide continuous pollutant time series having standard deviation that is close to that
481 observed.

482

483

484 **Acknowledgements**

485

486 Although this research was funded by the U.S. Environmental Protection Agency and approved
487 for publication, it does not necessarily reflect the Agency's views or policies. Two of the authors
488 (PSP and EG) acknowledge the support from the Coordinating research Council under contract
489 A-89.

490 **References**

- 491
- 492 Appel, K.W., Gilliland, A.B., Sarwar, G. and R.C. Gilliam. 2007. Evaluation of the Community
493 Multiscale Air Quality (CMAQ) model version 4.5: sensitivities impacting model performance
494 part I: ozone. *Atmos. Env.* 41 (40): 9603-9615.
495
- 496 Baklanov, A., Schlünzen, K., Suppan, P., Baldasano, J., Brunner, D., Aksoyoglu, S., Carmichael,
497 G., Douros, J., Flemming, J., Forkel, R., Galmarini, S., Gauss, M., Grell, G., Hirtl, M., Joffre, S.,
498 Jorba, O., Kaas, E., Kaasik, M., Kallos, G., Kong, X., Korsholm, U., Kurganskiy, A., Kushta, J.,
499 Lohmann, U., Mahura, A., Manders-Groot, A., Maurizi, A., Moussiopoulos, N., Rao, S. T.,
500 Savage, N., Seigneur, C., Sokhi, R. S., Solazzo, E., Solomos, S., Sørensen, B., Tsegas, G.,
501 Vignati, E., Vogel, B., and Y. Zhang, Y. 2014. Online coupled regional meteorology chemistry
502 models in Europe: current status and prospects, *Atmos. Chem. Phys.* 14: 317-398,
503 doi:10.5194/acp-14-317-2014.
504
- 505 Byun, D. W. and K.L. Schere. 2006. Review of the governing equations, computational
506 algorithms, and other components of the Models- 3 Community Multiscale Air Quality (CMAQ)
507 modeling system, *Appl. Mech. Rev.* 59: 51-77.
508
- 509 Civerolo, K., Hogrefe, C., Zalewsky, E., Hao, W., Sistla, G., Lynn, B., Rosenzweig, C. and P.L.
510 Kinney. 2010. Evaluation of an 18-year CMAQ simulation: Seasonal variations and long-term
511 temporal changes in sulfate and nitrate, *Atmos. Environ.*,
512 <http://dx.doi.org/10.1016/j.atmosenv.2010.06.056>.
513
- 514 Cohan, D.S. and R. Chen. 2014. Modeled and observed fine particulate matter reductions from
515 state attainment demonstrations, *J. Air & Waste Manage. Assoc.*, 64:9, 995-1002, DOI:
516 10.1080/10962247.2014.905509
517
- 518 Crooks, J. and V. Isakov. 2013. A wavelet-based approach to blending observations with
519 deterministic computer models to resolve the intraurban air pollution field, *J. Air & Waste
520 Manage. Assoc.* 1369-1385.
521
- 522 Delle Monache, L., Nipen, T, Deng, X., Zhou, Y. and R. Stull. 2006. Ozone ensemble forecasts:
523 2. A Kalman filter predictor bias correction, *J. Geophys. Res.*, 111, D05308,
524 doi:10.1029/2005JD006311.
525
- 526 Dennis, R., Fox, T., Fuentes, M., Gilliland, A., Hanna, S., Hogrefe, C., Irwin, J., Rao, S.T.,
527 Scheffe, R., Schere, K., Steyn, D., and A. Venkatram. 2010. A framework for evaluating
528 regional-scale numerical photochemical modeling systems. *Environ. Fluid Mech.* 10 (4): 471-
529 489.
530
- 531 Eder., B., Kang., D., Rao, S.T., Mathur, R., Yu, S., Otte, T, Schere, K., Wayland, R, Jackson, S.,
532 Davidson, P., McQueen, J. and G. Bridgers. 2010. Using national air quality forecast guidance
533 to develop local air quality index forecasts, *Bull. Amer. Meteor. Soc.* 313-326.
534

535 Foley, K., Reich, B.J., and S. Napelenok. 2012. Bayesian Analysis of a Reduced-Form Air
536 Quality Model, *Environ. Sci. Tech.* 46(14): 7604-7611.
537

538 Fuentes, M. and A.E. Raftery, 2005. Model Evaluation and Spatial Interpolation by Bayesian
539 Combination of Observations with Outputs from Numerical Models, *Biometrics.* 61: 36-45.
540

541 Galmarini, S., Rao, S.T. and D.G. Steyn. 2012. Preface, *Atm. Env.*, Volume 53, June, pp 1-3,
542 <http://dx.doi.org/10.1016/j.atmosenv.2012.03.001>.
543

544 Galmarini, S., Kioutsioukis, I. and E. Solazzo. 2013. *E pluribus unum*: ensemble air quality
545 predictions, *Atmos. Chem. Phys.* 13: 7153–7182.
546

547 Garcia, V.C., Foley, K.M., Gego, E., Holland, D. and S.T. Rao. 2010. A Comparison of
548 Statistical Techniques for Combining Modeled and Observed Concentrations to Create High-
549 Resolution Ozone Air Quality Surfaces, *J. Air & Waste Manage. Assoc.* 586-595.
550

551 Gery, M.W., Whitten, G. Z., Killus, J. P., and M.C. and M.C. Dodge. 1989. A photochemical
552 kinetics mechanism for urban and regional scale computer modeling, *J. Geophys. Res.* 94:
553 12925–12956.
554

555 Gilliland, A.B., Hogrefe, C., Pinder, R.W., Godowitch, J.M., Foley, K.M. and S.T. Rao. 2008.
556 Dynamic evaluation of regional air quality models: Assessing changes in O₃ stemming from
557 changes in emissions and meteorology. *Atmospheric Environment.* 42: 5110-5123.
558

559 Godowitch, J., Pouliot, G.A. and S.T. Rao. 2010. Assessing multi-year changes in modeled and
560 observed urban NO_x concentrations from a dynamic model evaluation perspective. *Atm. Env.*
561 doi:10.1016/j.atmosenv.2010.04.040.
562

563 Godowitch, J., Gilliam, R., and S.T. Rao. 2011. Diagnostic evaluation of ozone production and
564 horizontal transport in a regional photochemical air quality modeling system. *Atm. Env.* 45:
565 3977–3987.
566

567 Grell, G. A., Dudhia, J. and D. Stauffer. 1994. A Description of the Fifth-Generation
568 PennState/NCAR Mesoscale Model (MM5), NCAR Technical Note, NCAR/TN-398 + STR, 128
569 pp., available at: <http://nldr.library.ucar.edu/collections/technotes/asset-000-000-000-214.pdf>.
570

571 Hirst, D., Storvik, G. and A.R. Syversveen. 2003. A Hierarchical Modeling Approach to
572 Combining Environmental Data at Different Scales; *J. Royal Stat. Soc. Ser. C Appl. Stat.* 52:
573 377-390.
574

575 Hogrefe, C. and S.T. Rao. 2001. Demonstrating Attainment of the Air Quality Standards:
576 Integration of Observations and Model Predictions into the Probabilistic Framework. *J. Air &*
577 *Waste Manage. Assoc.* 51:1060-1072
578
579

580 Hogrefe, C., Lynn, B., Goldberg, R., Rosenzweig, C., Zalewsky, E., Hao, W., Doraiswamy, P.,
581 Civerolo, K., Ku, J.Y., Sistla, G. and P.L. Kinney. 2009. A Combined Model-Observation
582 Approach to Estimate Historic Gridded Fields of PM_{2.5} Mass and Species Concentrations, *Atm.*
583 *Env.*, doi:10.1016/j.atmosenv.2009.02.031
584
585 Hogrefe, C., Hao, W., Zalewsky, E., Ku, J.-Y., Lynn, B., Rosenzweig, C., Schultz, , M.G., Rast,
586 S., Newchurch, M., J., Wang, L, Kinney, P.L. and G. Sistla. 2010. An analysis of long-term
587 regional-scale ozone simulations over the Northeastern United States: variability and trends,
588 *Atmos. Chem. Phys.* 11: 567-582.
589
590 Hogrefe, C., Civerolo, K., Hao, W., Ku, J-Y, Zalewsky, E. and G. Sistla. 2012. Rethinking the
591 assessment of photochemical modeling systems in air quality planning applications, *Journal of*
592 *the Air & Waste Management Association*, Vol. 58 (8), 1086-1099, DOI:10.3155/1047-
593 3289.58.8.1086.
594
595 Hogrefe, C., S. Roselle, R. Mathur, Rao, S.T. and S. Galmarini. 2014. Space-time analysis of
596 the Air Quality Model Evaluation International Initiative (AQMEII) Phase 1 air quality
597 simulations, *Journal of the Air & Waste Management Association*, Vol. 64, Iss. 4,
598 DOI:10.1080/10962247.2013.811127
599
600 Houyoux, M. R., Vukovich, J. M., Coats, C. J., Wheeler, N. J. and P. Kasibhatla. 2000.
601 Emission inventory development and processing for the seasonal model for regional air quality,
602 *J. Geophys. Res.* 105: 9079–9090.
603
604 Jones, J.M., Hogrefe, C., Henry, R.F., Ku, J.Y. and G. Sistla. 2005. An assessment of the
605 sensitivity and reliability of the relative reduction factor approach in the development of 8-hr
606 ozone attainment plans. *J. Air & Waste Manage. Assoc.* 55(1): 13-19.
607
608 Junninen, H., Niska, H., Tuppurainen, K., Ruuskanen, J. and M.Kolehmainen. 2004. Methods
609 for imputation of missing values in air quality data sets. *Atmospheric Environment.* 38: 2895–
610 2907
611
612 Kang, D., Mathur, R., Rao, S.T. and S. Yu. 2008. Bias adjustment techniques for improving
613 ozone air quality forecasts. *J. Geophys. Res.* 113.
614
615 Kang, D., Mathur, R. and and S.T. Rao. 2010. Real-time bias-adjusted O₃ and PM_{2.5} air quality
616 index forecasts and their performance evaluations over the continental United States, *Atm. Env.*
617 2203-2212.
618
619 Kang, D., Hogrefe, C., Foley, K., Napelenok, S., Mathur, R. and S.T. Rao. 2013. Application of
620 the Kolmogorov-Zurbenko filter and the decoupled direct 3D method for the dynamic evaluation
621 of a regional air quality model. *Atm. Env.* 80: 58-69
622
623

624 Kulkarni, S., Kaduwela, A., Avise, J., DaMassa, J. and D. Chau. 2014. An extended approach
625 to calculate the ozone response factors used in attainment demonstration for the national ambient
626 air quality standards. *Journal of the Air & Waste Management Association*. 64 (10): 1204-1213,
627 DOI:10.1080/10962247.2014.936984.

628

629 Lin, S., Jones, R., Pantea, C., Ozkaynak, H., Rao, S.T., Hwang, S. and V. Garcia. 2013. Impact
630 of NO_x Emission Reduction Policy on Hospitalizations for Respiratory Disease in New York
631 State. *J. of Exposure Science and Environmental Epidemiology*. 73-80.

632

633 McMillan, N.; Holland, D.M.; Morara, M. and J. Feng. 2010. Combining Numerical Model
634 Output and Particulate Data Using Bayesian Space-Time Modeling; *Environmetrics*. 2: 48-65.

635

636 Napelenok, S.L., Foley, K.M., Kang, D., Mathur, R., Pierce, T. and S.T. Rao. 2011. Dynamic
637 evaluation of regional air quality model's response to emissions in the presence of uncertain
638 emission inventories. *Atmos. Env.* 45: 4091-4098.

639

640 NRC. 1994. *Science and Judgment in Risk Assessment (NRC Blue Book)*. Washington, DC:
641 The National Academies Press.

642

643 Pegues, A.H., Cohan, D.S., Digar, A., Douglass, C., and R.S. Wilson. 2012. Efficacy of recent
644 state implementation plans for 8-hour ozone. *J. Air & Waste Manage. Assoc.* 62(2): 252-261.

645

646 Pierce, T., Geron, C., Bender, L., Dennis, R., Tonnesen, G. and A. Guenther. 1998. Influence of
647 Increased Isoprene Emissions on Regional Ozone Modeling; *J. Geophys. Res.* 103: 25611-
648 25629.

649

650 Rao, S.T., Zurbenko, I., Neagu, R., Porter, P.S., Ku, J.Y. and R. Henry. 1997. Space and Time
651 Scales in Ambient Ozone Data, *Bull. of the Amer. Meteor. Soc.* 78(10): 2153-2166.

652

653 Rao, S.T. and I.G. Zurbenko. 1994. Detecting and tracking changes in ozone air quality. *Journal*
654 *of the Air and Waste Management Association*. 44: 1089-1092.

655

656 Rao, S.T., Galmarini, S. and K. Puckett. 2011. Air Quality Model Evaluation International
657 Initiative (AQMEII), *Bull. Amer. Meteor. Soc.* 23-30.

658

659 Reich, B.J., Cooley, D., Foley, K., Napelenok, S., and B.A. Shaby. 2013. Extreme Value
660 Analysis for Evaluating Ozone Control Strategies. *Annals of Appl. Stat.* 7(2): 739-762

661

662 Schulz, M. G., ed. 2010. RETRO final report: REanalysis of the TROpospheric chemical
663 composition over the past 40 years – A long-term global modeling study of tropospheric
664 chemistry, Reports on Earth System Science, edited by: available at: [http://retro.](http://retro.enes.org/reports/RETRO%20Final%20Report.pdf)
665 [enes.org/reports/RETRO Final Report.pdf](http://retro.enes.org/reports/RETRO Final Report.pdf), last access: 30 August 2010, Max Planck Institute for
666 Meteorology, Hamburg, report no. 48/2007, ISSN 1614-1199, August 2007.

667

668 Simon, H., Baker, K.R. and S. Phillips. 2012. Compilation and interpretation of photochemical
669 model performance statistics published between 2006 and 2012, *Atmospheric Environment*, 61,
670 124-139, <http://dx.doi.org/10.1016/j.atmosenv.2012.07.012>
671

672 Sistla, G., Hogrefe, C., Hao, W., Ku, J.Y., Zalewsky, E., Henry, R.F., and K. Civerolo. 2004. An
673 operational assessment of the application of the relative reduction factors in the demonstration of
674 the attainment of the 8-hr ozone national ambient air quality standard. *J. Air & Waste Manage.*
675 *Assoc.* 54(8): 950-959.
676

677 USEPA. 2014. Air Quality Modeling Technical Support Document: Tier 3 Motor Vehicle
678 Emission and Standards; Air Quality Assessment Division, Office of Air Quality Planning and
679 Standards, U.S. Environmental Protection Agency, Research Triangle Park, NC, EPA-454/R-14-
680 002, 128 pp.
681

682 Wang, L. and W. Chen. 2014. Equiratio cumulative distribution function matching as an
683 improvement to the equidistant approach in bias correction of precipitation *Atmos. Sci. Let.* 15:
684 1–6, Published online 31 July 2013 in Wiley Online Library (wileyonlinelibrary.com) DOI:
685 10.1002/asl2.454.

686 **Legend for Tables**

687

688 Table 1: Domain-wide mean metric of 4HDM8O3 predictions for all base year – target year
689 pairs. Values in brackets are 95% confidence intervals

690

691 Table 2: Multiple comparisons of adjustment methods (95% level)

692

693 Table 3: Percent of base- / prediction- year pairs where a given method is better according to a
694 particular metric. Example for MAB: MV is better than CMAQ (73% of pairs)
695 and RATIO (58% of pairs).

696

697 Table 4. Effect of averaging the largest values for a given year. Each set of average values
698 begins with the largest observed. For example, ‘1’ means the largest while ‘3’
699 means the 3 largest.

700

701

702 **Legend for Figures**

703

704 Fig.1: Ratios of future year (2004) to base year (2001) 4th highest daily maximum 8-hr ozone
705 concentrations extracted from the observations and CMAQ output.

706

707 Fig. 2: Domain-wide statistics in predicting future 4HDM8O3 concentrations using 1996 as the
708 base year for raw CMAQ output, RATIO approach, and the four new methods introduced in this
709 study. a) RMSE (ppb), b) MAB (ppb), and c) Correlation.

710

711 Fig. 3: Spatial image of RSME (in ppb) in predicted 4HDM8O3 concentrations for all base
712 year/prediction year combinations from each method.

713

714 Fig. 4: Fraction of sites predicted 4HDM8O3 concentrations fall within a given distance from
715 observations

716

717 Fig. 5: RSME (in ppb) for the 2004 daily maximum 8-hr ozone concentrations using 2001 as the
718 base year for the upper half of the distribution of daily maximum 8-hr ozone concentrations.

719

720 Fig. 6: Change in daily maximum 8-hr ozone distributions between 2001 base year and 2004
721 prediction year for each method: a) Change in the upper half of the frequency distribution; b)
722 change in the 98th percentile (changes in the CDF2 method are the same as CMAQ).

723

724 Fig. 7: Domain-wide statistics for same year predictions: a) mean absolute bias, b) standard
725 deviation, c) correlation coefficient. Note that no results are shown for the RATIO and CDF2
726 approaches. For the RATIO approach, the same year ratio of model predictions is equal to one
727 and, thus, the same year predicted value equals the observed value, and for the CDF2 approach,
728 the same year predicted value equals that for the CDF1 approach.

729

730 Fig. 8: Mean bias of same-year predictions by percentiles. a) 2001, b) 2004.

731 **Table 1. Domain-wide mean metric of 4HDM8O3 predictions for all base year – target year pairs. Values in brackets are**
 732 **95% confidence intervals**
 733
 734

| Metric | Method | | | | | |
|---------------------------|---------------------------|----------------------------|---------------------------|----------------------------|---------------------------|---------------------------|
| | RATIO | CMAQ | MV | TC | CDF1 | CDF2 |
| MAB (ppb) | 7.48 [7.39 7.57] | 8.31 [8.07 8.54] | 7.26 [7.18 7.36] | 7.06 [6.96 7.17] | 7.00 [6.89 7.05] | 6.90 [6.82 6.98] |
| RMSE (ppb) | 9.49 [9.38 9.60] | 10.35 [10.08 10.62] | 9.25 [9.14 9.37] | 9.81 [9.52 10.17] | 8.91 [8.81 9.02] | 8.71 [8.62 8.81] |
| FMAB (%) | 8.7 [8.6 8.8] | 9.6 [9.3 9.9] | 8.5 [8.4 8.6] | 8.2 [8.1 8.3] | 8.1 [8.0 9.2] | 8.1 [8.0 8.2] |
| FRMSE (%) | 11.1 [11.0 11.2] | 11.8 [11.5 12.1] | 10.7 [10.6 10.8] | 11.4 [11.1 11.8] | 10.5 [10.4 10.6] | 10.3 [10.2 10.4] |
| R2 | 0.26 [0.245 0.272] | 0.32 [0.281 0.353] | 0.31 [0.300 0.328] | 0.29 [0.267 0.306] | 0.33 [0.316 0.344] | 0.32 [0.306 0.333] |
| Index of agreement | 0.78 [0.772 0.785] | 0.77 [0.750 0.780] | 0.81 [0.799 0.811] | 0.79 [0.776 0.799] | 0.82 [0.811 0.821] | 0.81 [0.802 0.813] |

735
 736
 737
 738
 739
 740
 741
 742
 743
 744
 745
 746
 747
 748
 749
 750

751 **Table 2. Multiple comparisons of adjustment methods (95% level)**

752

| | <u>MAB</u> | <u>RMSE</u> |
|---------------------|--|---|
| RATIO < > | CMAQ MV, TC, CDF1, CDF2 | CMAQ, TC CDF1, CDF2 |
| CMAQ < > | NONE ALL | NONE RATIO, MV, CDF1, CDF2 |
| MV < > | RATIO , CMAQ TC, CDF1, CDF2 | CMAQ, TC CDF2 |
| TC < > | RATIO, CMAQ, MV NONE | NONE RATIO, MV, CDF1, CDF2 |
| CDF1 < > | RATIO, CMAQ, MV NONE | RATIO, CMAQ, TC NONE |
| CDF2 < > | RATIO, CMAQ, MV NONE | RATIO, CMAQ, MV, TC NONE |

753

**Table 3. Percent of base- / prediction- year pairs where a given method is better according to a particular metric.
 Example for MAB: MV is better than CMAQ (73% of pairs) and RATIO (58% of pairs).**

| | <u>CMAQ</u> | <u>RATIO</u> | <u>MV</u> | <u>TC</u> | <u>CDF1</u> | <u>CDF2</u> |
|--------------------|-------------|--------------|-----------|-----------|-------------|-------------|
| <u>MAB</u> | | | | | | |
| CMAQ | | 36 | 27 | 27 | 23 | 17 |
| RATIO | 64 | | 42 | 32 | 16 | 17 |
| MV | 73 | 58 | | 46 | 38 | 27 |
| TC | 73 | 68 | 54 | | 43 | 34 |
| CDF1 | 77 | 84 | 62 | 57 | | 30 |
| CDF2 | 83 | 83 | 73 | 66 | 70 | |
| <u>RMSE</u> | | | | | | |
| CMAQ | | 47 | 30 | 46 | 28 | 20 |
| RATIO | 53 | | 38 | 44 | 18 | 11 |
| MV | 70 | 62 | | 54 | 37 | 26 |
| TC | 54 | 56 | 46 | | 42 | 32 |
| CDF1 | 72 | 82 | 63 | 58 | | 31 |
| CDF2 | 80 | 89 | 74 | 68 | 69 | |
| <u>R2</u> | | | | | | |
| CMAQ | | 52 | 38 | 48 | 39 | 19 |
| RATIO | 48 | | 34 | 38 | 16 | 04 |
| MV | 62 | 66 | | 46 | 37 | 19 |
| TC | 52 | 62 | 54 | | 42 | 28 |
| CDF1 | 61 | 84 | 63 | 58 | | 20 |
| CDF2 | 81 | 96 | 81 | 72 | 80 | |

Table 4. Effect of averaging the largest values for a given year. Each set of average values begins with the largest observed. For example, '1' means the largest while '3' means the 3 largest.

| <u>number in average:</u> | <u>1</u> | <u>2</u> | <u>3</u> | <u>4</u> | <u>5</u> | <u>6</u> | <u>7</u> | <u>8</u> | <u>9</u> | <u>10</u> | <u>4th highest</u> |
|----------------------------------|-----------------|-----------------|-----------------|-----------------|-----------------|-----------------|-----------------|-----------------|-----------------|------------------|--------------------------------------|
| <u>mean absolute bias</u> | | | | | | | | | | | |
| RATIO | 12.71 | 10.75 | 9.44 | 8.57 | 7.94 | 7.49 | 7.15 | 6.88 | 6.66 | 6.47 | 7.48 |
| CMAQ | 11.99 | 10.78 | 9.90 | 9.26 | 8.77 | 8.37 | 8.05 | 7.79 | 7.55 | 7.35 | 8.31 |
| MV | 11.07 | 9.66 | 8.74 | 8.15 | 7.70 | 7.37 | 7.11 | 6.89 | 6.72 | 6.56 | 7.26 |
| TC | 10.95 | 9.46 | 8.53 | 7.92 | 7.45 | 7.11 | 6.85 | 6.63 | 6.46 | 6.30 | 7.06 |
| CDF1 | 10.96 | 9.47 | 8.52 | 7.89 | 7.44 | 7.10 | 6.83 | 6.60 | 6.42 | 6.25 | 7.00 |
| CDF2 | 10.28 | 8.98 | 8.16 | 7.62 | 7.24 | 6.96 | 6.73 | 6.55 | 6.39 | 6.26 | 6.90 |
| <u>RMSE</u> | | | | | | | | | | | |
| RATIO | 16.12 | 13.62 | 11.90 | 10.78 | 9.99 | 9.43 | 9.01 | 8.68 | 8.41 | 8.19 | 9.49 |
| CMAQ | 14.88 | 13.29 | 12.11 | 11.32 | 10.72 | 10.26 | 9.89 | 9.58 | 9.31 | 9.07 | 10.35 |
| MV | 14.05 | 12.26 | 11.08 | 10.31 | 9.74 | 9.32 | 8.99 | 8.73 | 8.50 | 8.31 | 9.25 |
| TC | 14.60 | 12.80 | 11.66 | 10.91 | 10.35 | 9.93 | 9.60 | 9.33 | 9.11 | 8.91 | 9.81 |
| CDF1 | 13.90 | 12.03 | 10.82 | 10.02 | 9.45 | 9.023 | 8.69 | 8.41 | 8.19 | 7.99 | 8.91 |
| CDF2 | 12.97 | 11.36 | 10.31 | 9.62 | 9.13 | 8.77 | 8.49 | 8.26 | 8.07 | 7.91 | 8.71 |
| <u>R²</u> | | | | | | | | | | | |
| RATIO | 0.22 | 0.29 | 0.35 | 0.39 | 0.42 | 0.45 | 0.47 | 0.48 | 0.49 | 0.50 | 0.26 |
| CMAQ | 0.31 | 0.36 | 0.40 | 0.42 | 0.44 | 0.45 | 0.46 | 0.47 | 0.48 | 0.48 | 0.32 |
| MV | 0.27 | 0.34 | 0.39 | 0.43 | 0.46 | 0.4 | 0.49 | 0.50 | 0.51 | 0.52 | 0.31 |
| TC | 0.26 | 0.33 | 0.38 | 0.41 | 0.43 | 0.45 | 0.46 | 0.48 | 0.48 | 0.49 | 0.29 |
| CDF1 | 0.28 | 0.36 | 0.41 | 0.45 | 0.48 | 0.50 | 0.52 | 0.53 | 0.54 | 0.55 | 0.33 |
| CDF2 | 0.29 | 0.36 | 0.41 | 0.44 | 0.47 | 0.48 | 0.50 | 0.51 | 0.52 | 0.52 | 0.32 |

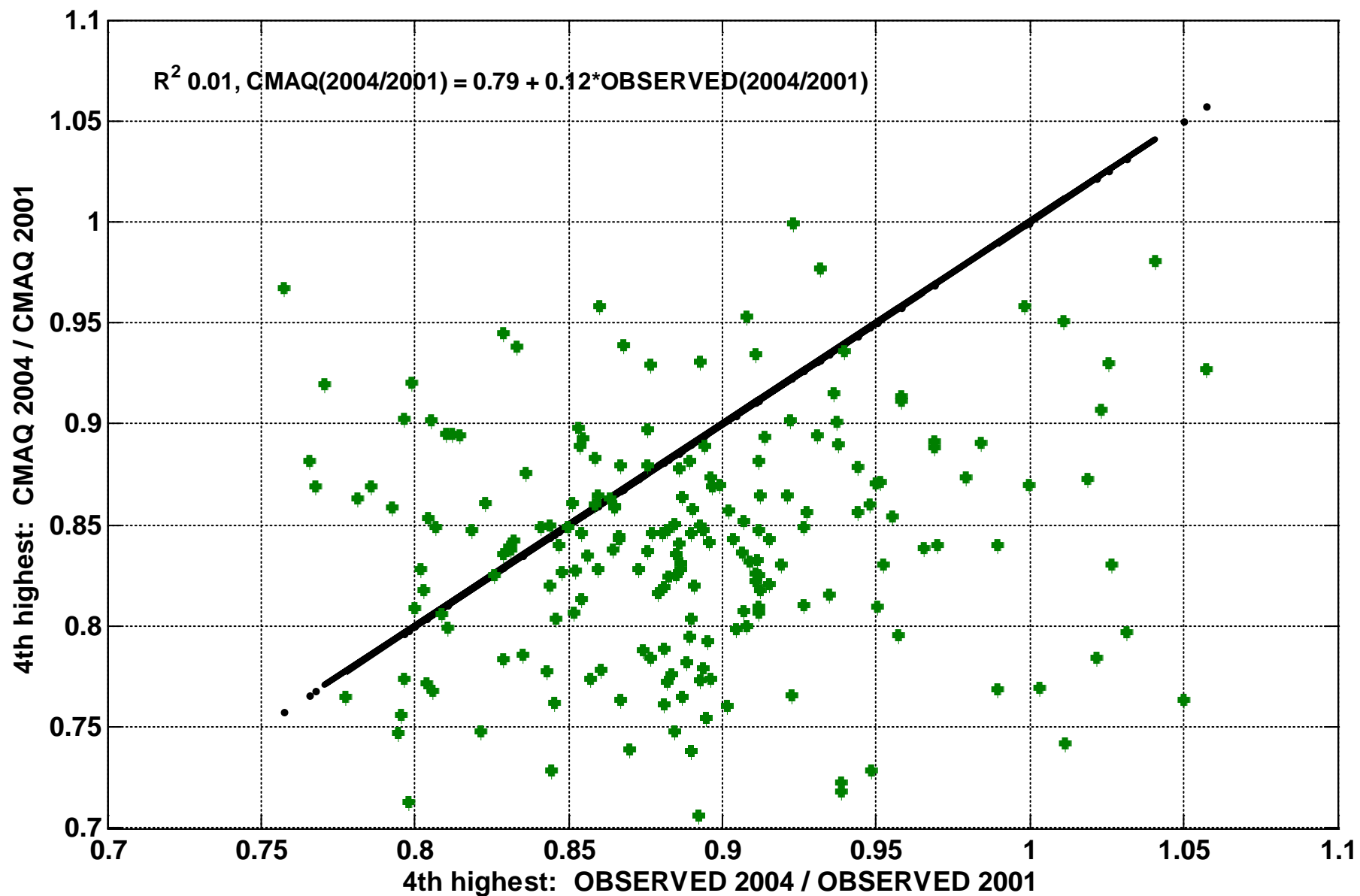


Fig. 1: Ratios of future year (2004) to base year (2001) 4th highest daily maximum 8-hr ozone concentrations extracted from the observations and CMAQ output.

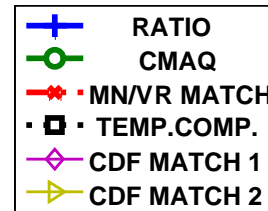
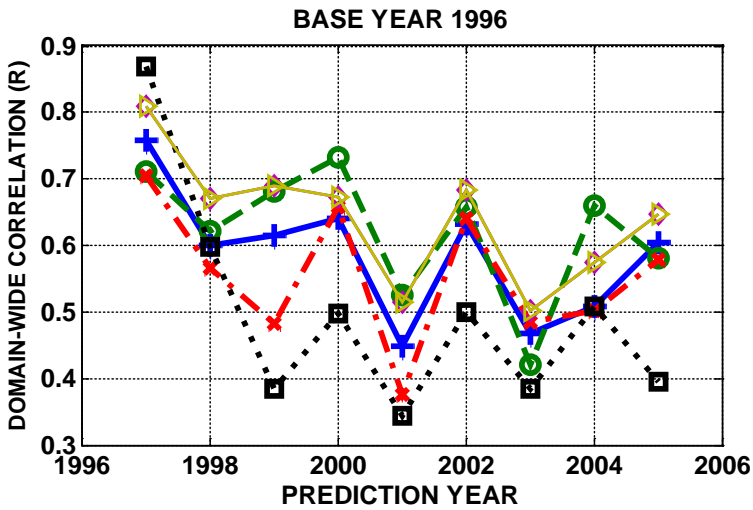
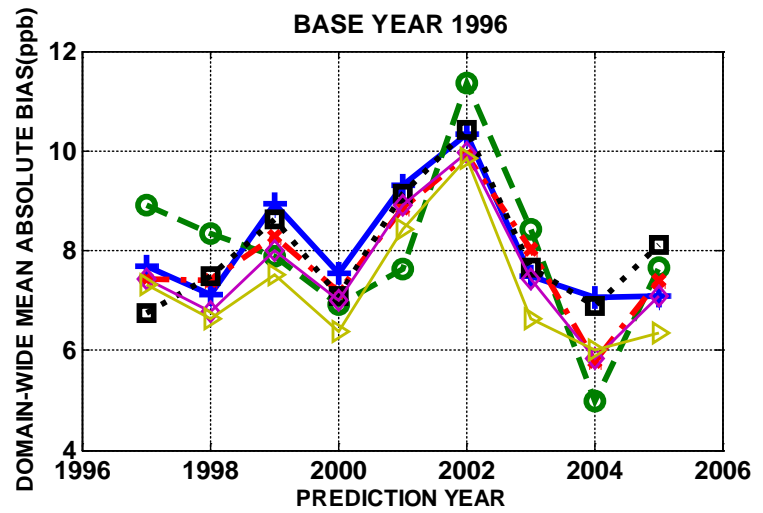
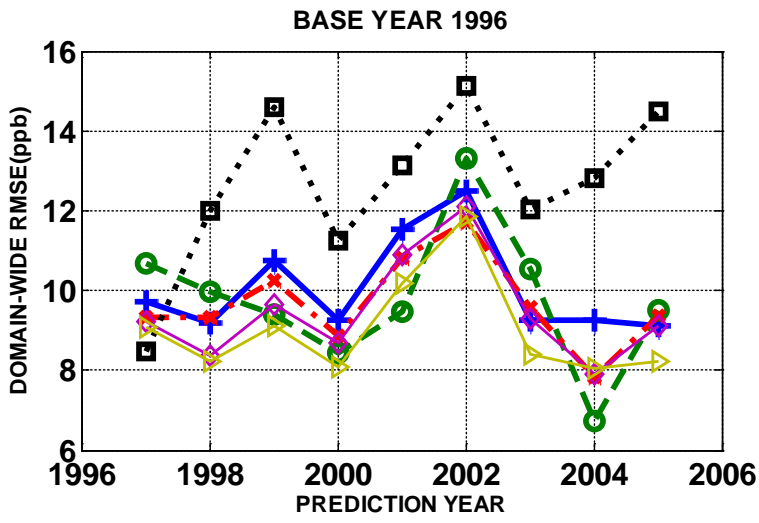


Fig. 2. Domain-wide statistics in predicting future 4HDM8O3 concentrations using 1996 as the base year for raw CMAQ output, RATIO approach, and the four new methods introduced in this study. a) RMSE (ppb), b) MAB (ppb), and c) correlation

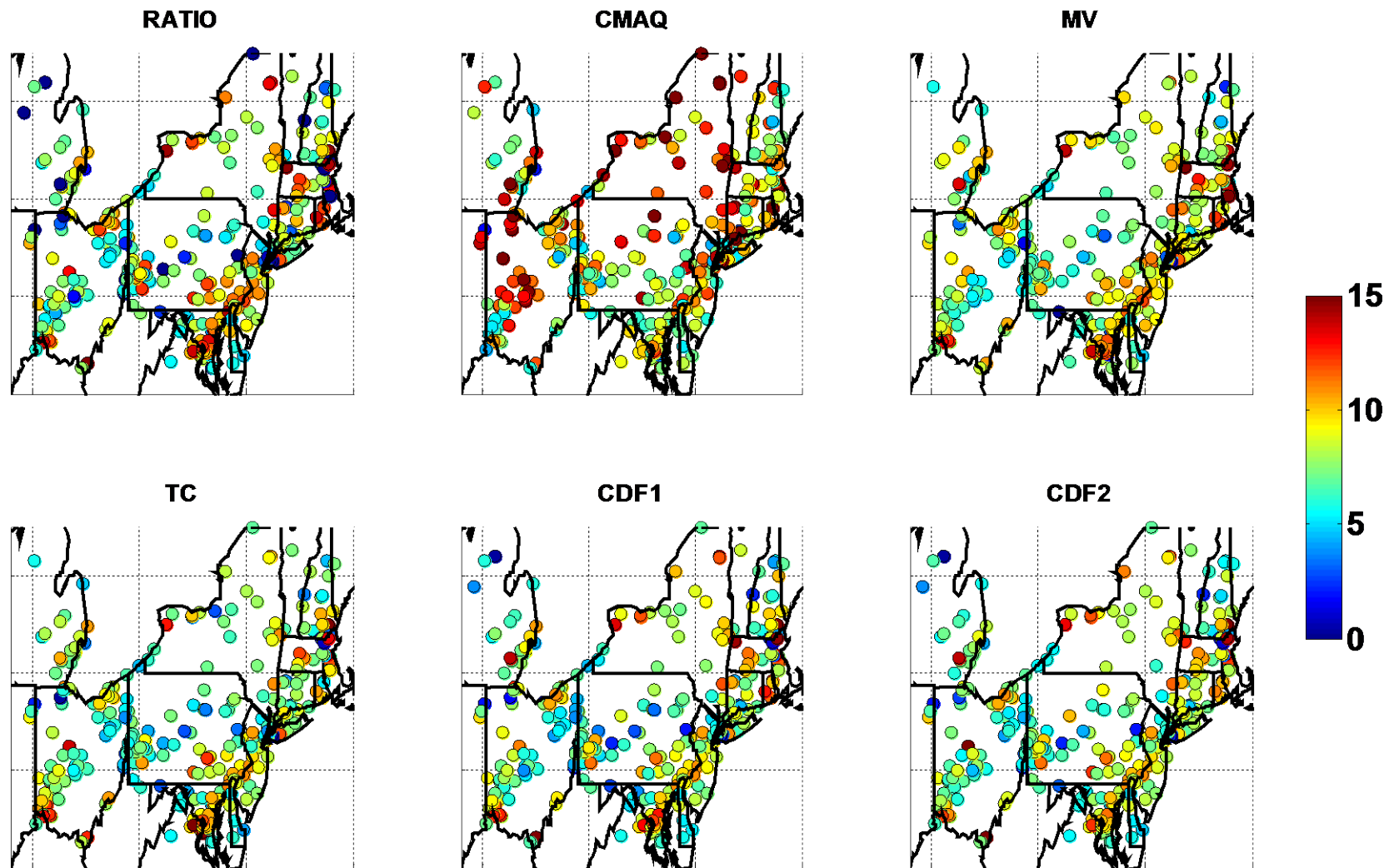


Fig. 3: Spatial image of RSME (in ppb) in predicted 4HDM8O3 concentrations for all base year/prediction year combinations from each method.

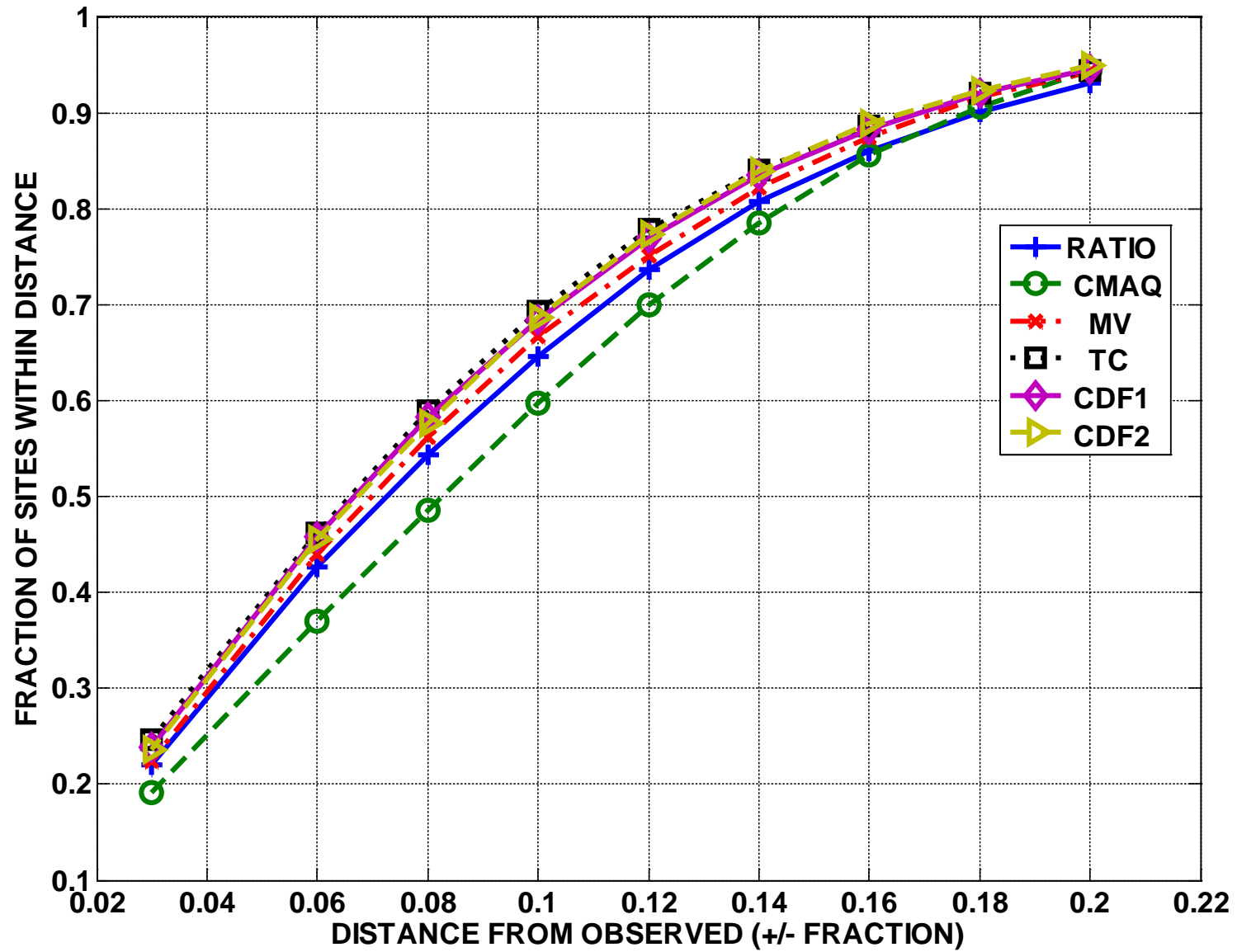


Fig. 4: Fraction of times predicted 4HDM8O3 concentrations fall within a given distance from observations

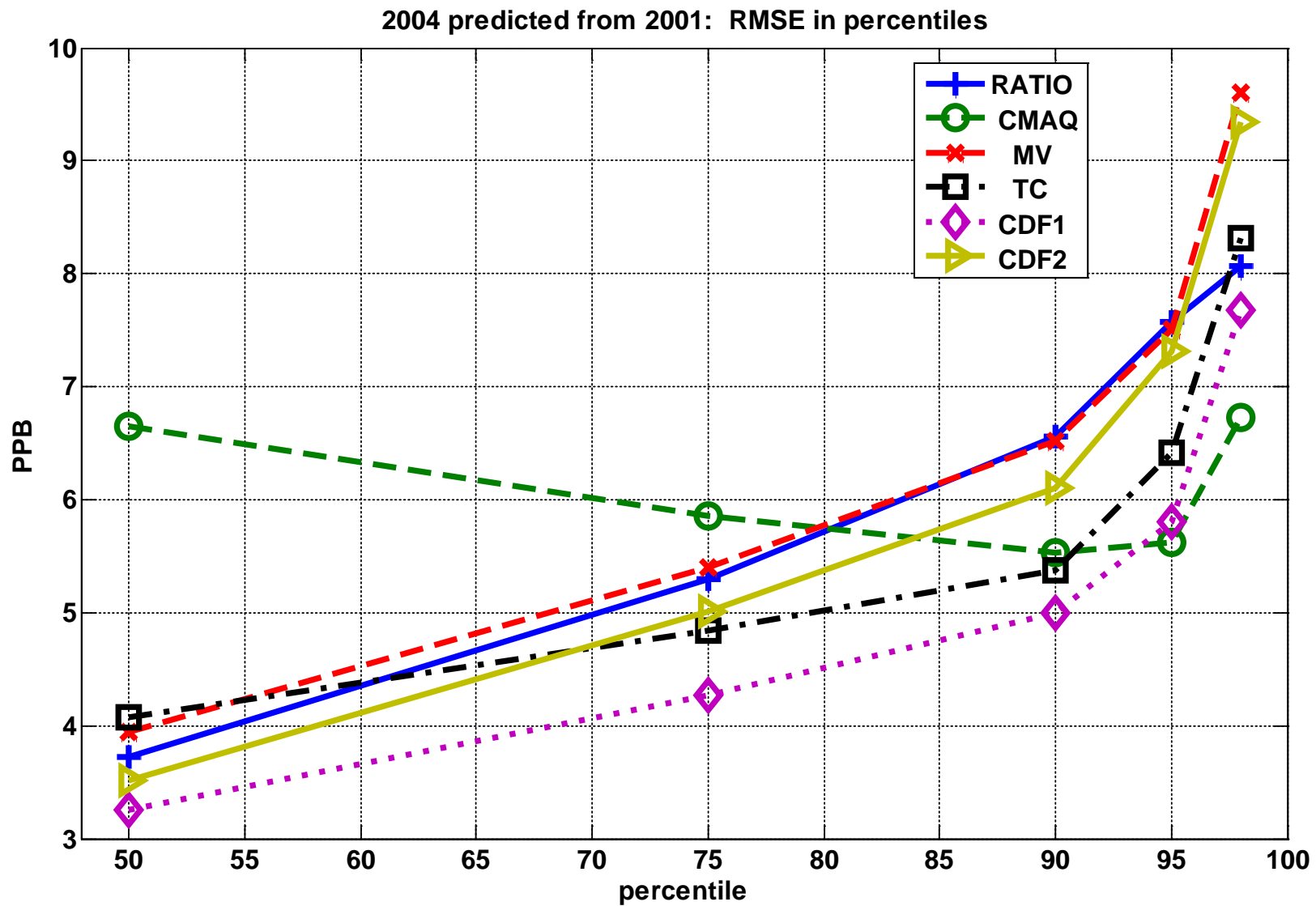


Fig. 5: RSME (in ppb) for the 2004 daily maximum 8-hr ozone concentrations using 2001 as the base year for the upper half of the distribution of daily maximum 8-hr ozone concentrations.

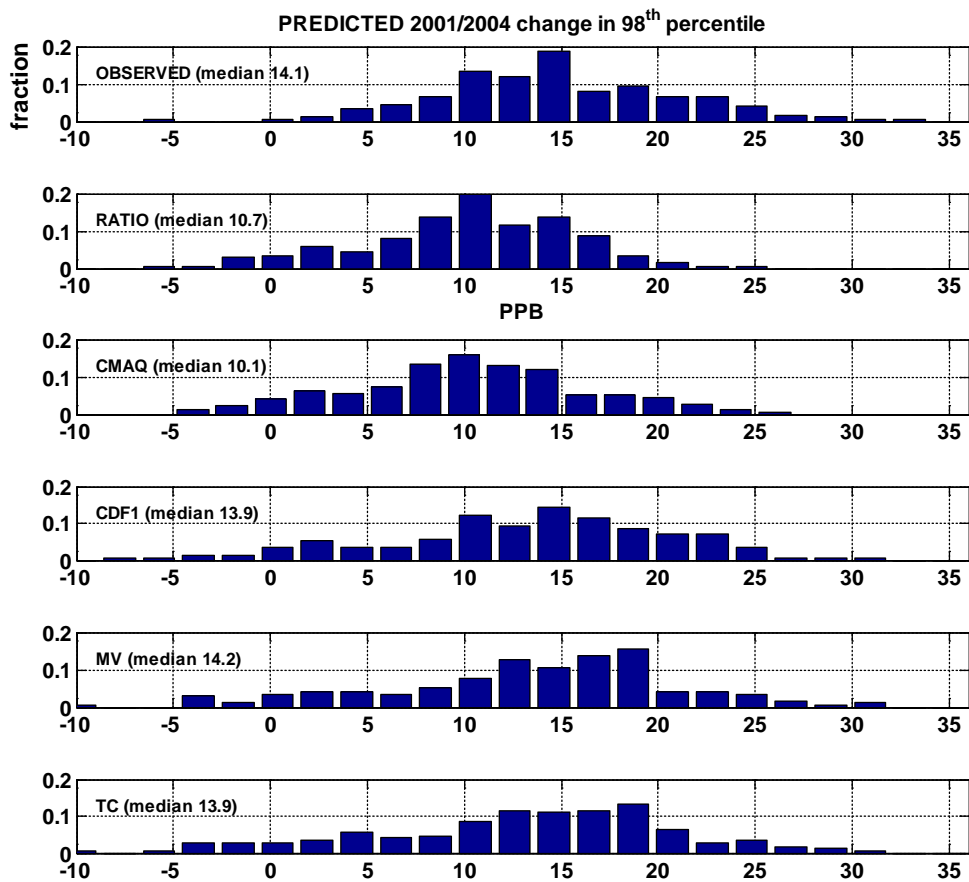
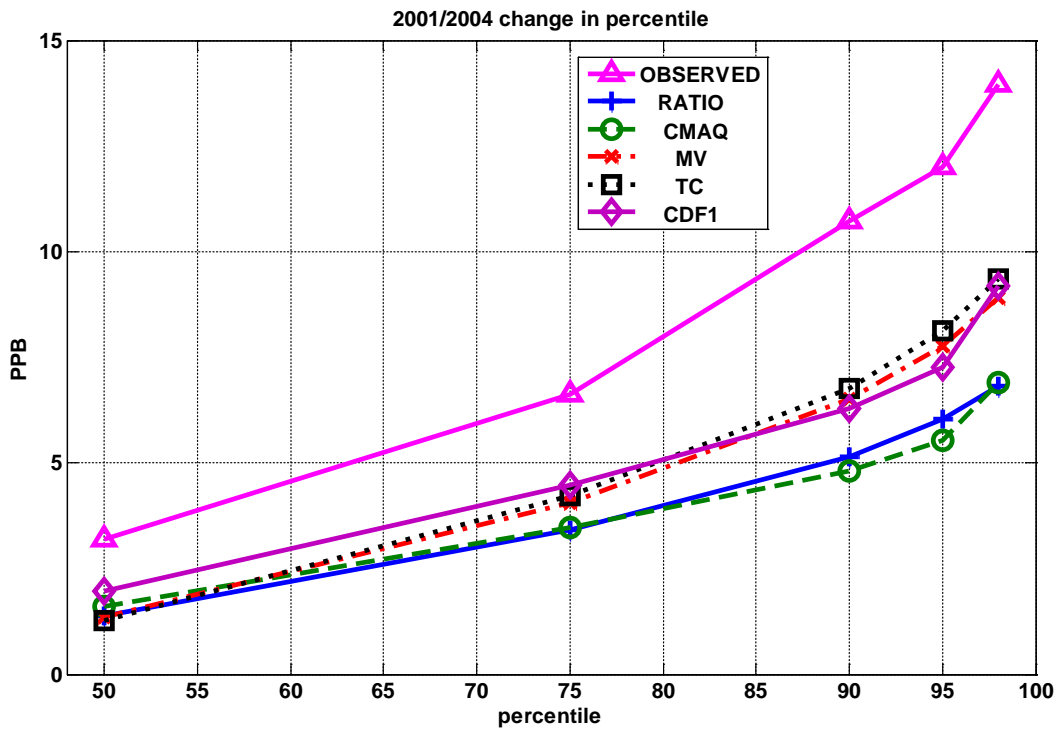


Fig. 6: Change in daily maximum 8-hr ozone distributions between 2001 base year and 2004 prediction year for each method: a) Change in the upper half of the frequency distribution; b) change in the 98th percentile (changes in the CDF2 method are the same as CMAQ).

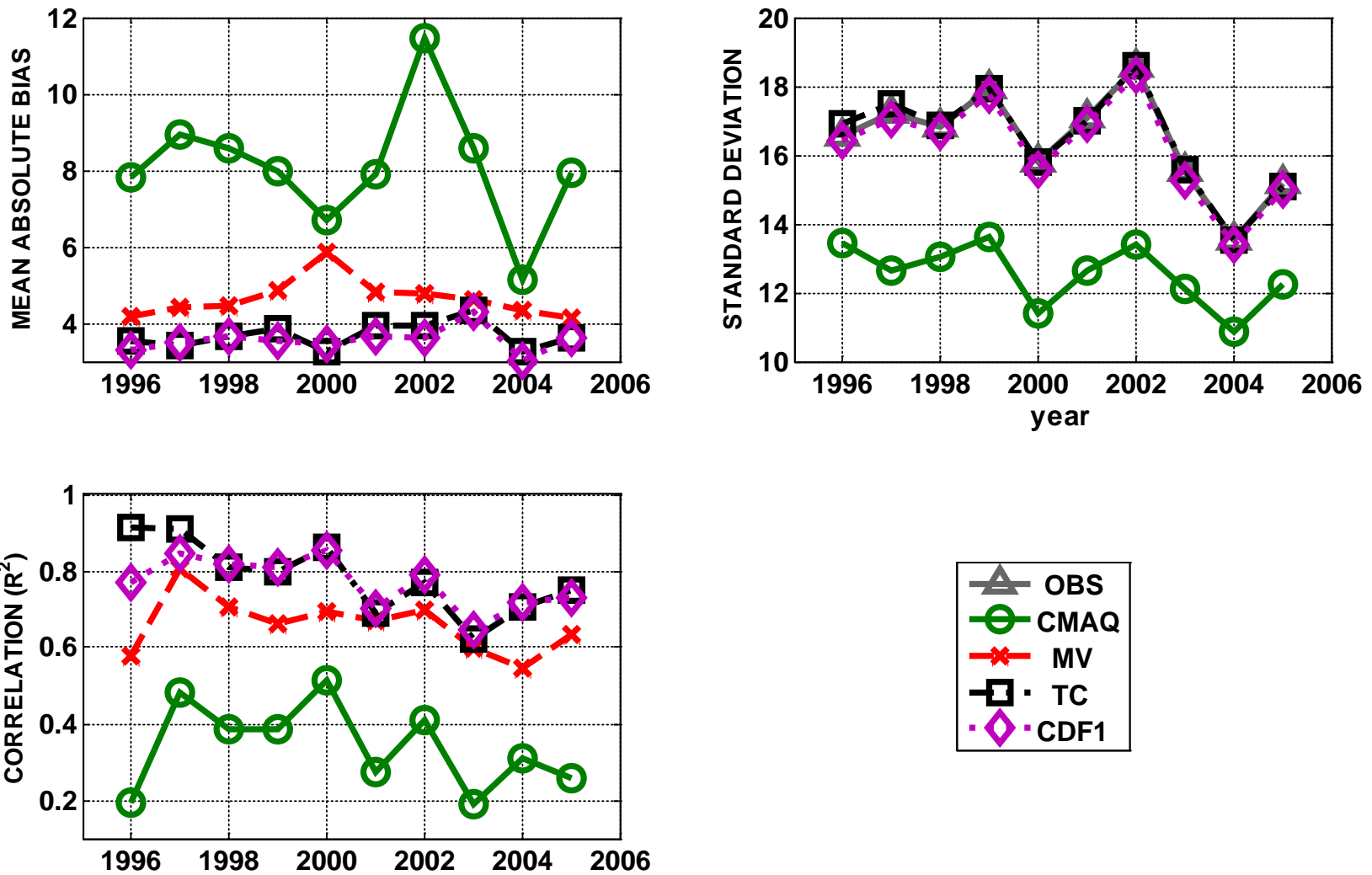


Fig 7: Domain-wide mean metrics for using same-year CMAQ adjustments (methods applied and compared with observations for a single year): a) mean absolute bias of annual 4th highest 8-hour daily maximum (4HDM8O3), b) standard deviation of 8-hour daily maximum, c) correlation coefficient (R^2) between observed and adjusted 4HDM8O3. Note that no results are shown for the RATIO and CDF2 approaches. For the RATIO approach, the same year ratio of model predictions is equal to one and, thus, the same year predicted value equals the observed value, and for the CDF2 approach, the same year predicted value equals that for the CDF1 approach.

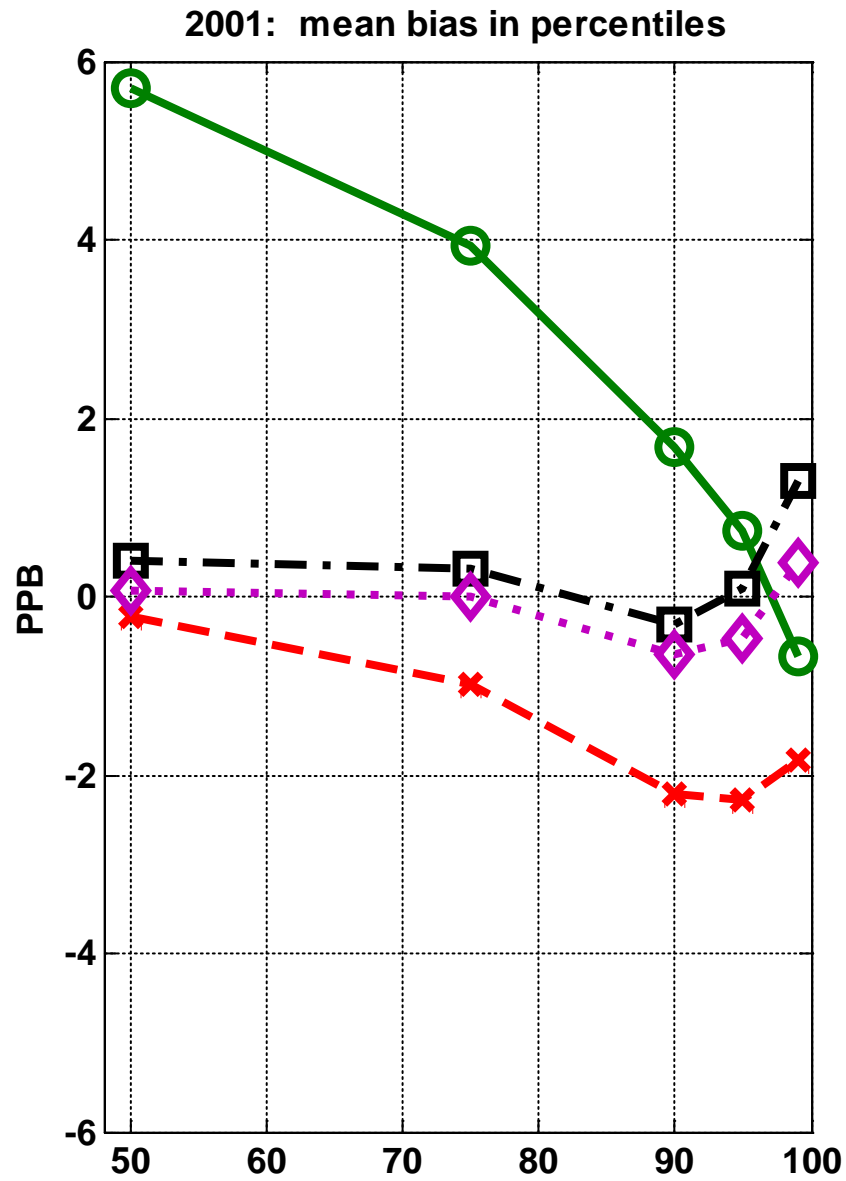
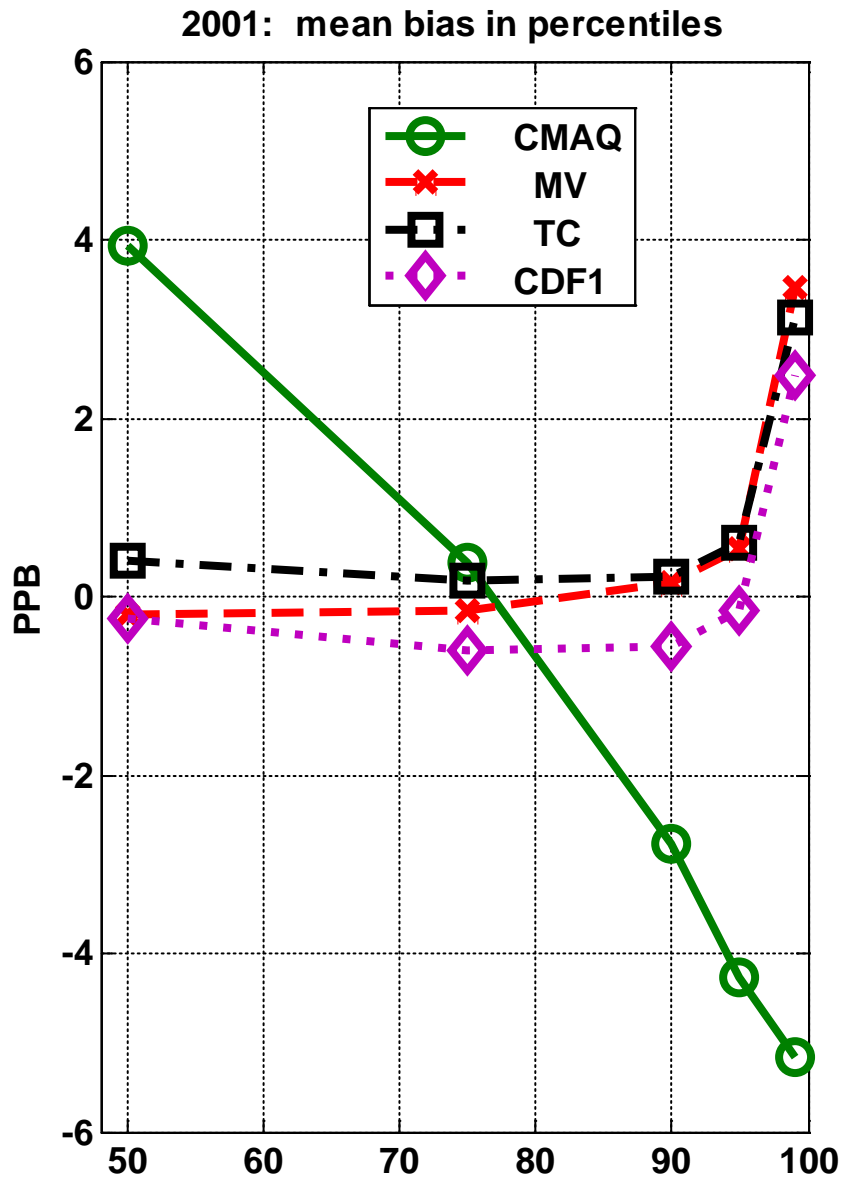


Fig. 8: Mean bias of same-year predictions by percentiles. a) 2001, b) 2004